Computation of eco-driving cycles for Hybrid Electric Vehicles: Comparative analysis

D. Maamria[a,*], K. Gillet[a], G. Colin[a], Y. Chamaillard[a], C. Nouillant[b]

[a]*Univ. Orléans, PRISME, EA 4229, F45072, Orléans, France.*
djamaleddine.maamria@gmail.com, (kristan.gillet, guillaume.colin,
yann.chamaillard)@univ-orleans.fr
[b]*PSA Peugeot Citroën, Direction Recherche Innovation & Technologies Avancées
(DRIA), France.* cedric.nouillant@mpsa.com

Abstract

In this paper, the calculation of eco-driving cycles for a Hybrid Electric Vehicle (HEV), using Dynamic Programming (DP), is investigated from the solving method complexity viewpoint. The study is based on a comparative analysis of four optimal control problems formulated using distinct levels of modeling. Starting with three state dynamics (vehicle position and speed, battery state-of-charge) and three control variables (engine and electric machine torque, gear-box ratio), the number of state variables is reduced to two in a first simplification. The other two simplifications are based on decoupling the optimization of the control variables into two steps: an eco-driving cycle is calculated supposing that the vehicle is propelled only by the engine. Then, assuming that the vehicle follows the eco-driving cycle calculated in the first step, an off-line energy management strategy (torque split) for an HEV is calculated to split the requested power at the wheels between the electric source and the engine. As is shown, the decreased complexity and the

---

*Corresponding author.

decoupling optimization lead to a sub-optimality in fuel economy while the computation time is noticeably reduced. Quantitative results are provided to assess these observations.

1. Introduction

Spurred by environmental requirements, economic factors and energy-saving interests, eco-driving has attracted much attention from the scientific community in the last decade. It is now considered as a major solution to reduce the energy consumption linked to transportation. It can be seen as a multi-criteria optimization (fuel consumption, duration, drivability, etc) of various tasks (navigation, guidance, stabilization) under safety constraints. In other words, the idea of eco-driving is to calculate the vehicle velocity trajectory that minimizes the vehicle energy consumption under constraints: speed limitations, final time and total traveled distance. This question can be solved using optimal control tools.

For conventional vehicles, fuel consumption, engine emissions or any combination of both over a fixed time window is the cost function to be minimized (Mensing et al., 2011, 2014). For full electric cars, the cost function to be minimized is the electric power requested by the electric machine (Dib et al., 2014; Petit and Sciarretta, 2011; F. Mensing, 2013; Sciarretta et al., 2015; Miyatake et al., 2011). The duration of the trip can be considered as an additional degree of freedom in the optimization. A trade-off between the

2

fuel consumption and the duration can be found. Two dynamics are usually considered: the position and the speed of the vehicle. For these two architectures (conventional and electric), two control variables are used: the engine or the electric machine torque and the gear-box ratio while the main constraints bear on speed limitations, vehicle stops and total traveled distance (F. Mensing, 2013; Sciarretta et al., 2015)

However, having an additional energy source increases the complexity of the models and thus the algorithms used to calculate eco-driving cycles as mentioned in (van Keulen et al., 2010). In the case of hybrid electric vehicles, additional state and control variables have to be considered in the optimization: the battery State Of Charge (SOC) with a constraint on its final value and the electric machine torque.

The work in (Kim et al., 2009) presents a strategy that optimizes both the speed profile and the torque split between the electric machine and the engine using a Gradient method. More recently, the algorithms in (F. Mensing, 2013; Ngo et al., 2010) combine dynamic programming with the Energy Management System (EMS) design for a Hybrid Electric Vehicle (HEV) to calculate eco-driving cycles. A bi-level approach that reduces computation time was suggested in (Ngo et al., 2010). The optimal control strategy is calculated by decoupling the optimization of the control variables. In a first step (an outer loop) the speed trajectory is optimized assuming that the vehicle is propelled only by the internal combustion engine or the electric machine. In a second step, the power split between the engine and the electric machine is optimized in an inner loop for a given vehicle speed, gear-box ratio and wheel torque. The missing point is the quantification of the sub-optimality induced

by the method used. A similar approach was used in (Sciarretta et al., 2015) where an overview of eco-driving problems for various architectures (electric, conventional and hybrid electric cars) was given. Analytical solutions were suggested in the case where the gear-box ratios are not optimized.

Later, in (Heppeler et al., 2014), the authors worked on the direct optimization of the EMS for an HEV with a small deviation from the given desired vehicle velocity as an additional degree of freedom. It was shown that the additional degree of freedom for the velocity decreases fuel consumption by about 6.8% compared to a real-time power split strategy and by about 4.3% compared to an off-line power split algorithm with a *fixed* velocity trajectory. The work in (Bouvier et al., 2015) compared two approaches to calculate eco-driving cycles for a parallel HEV in terms of fuel saving. The study concluded that in order to generate the best speed trajectory in terms of fuel consumption, it is necessary to consider that the vehicle is an HEV: this consideration saves up to 3%. However, the comparison of the computation time of the two methods was not investigated.

This paper follows the path described above and pursues the analysis further. A parallel HEV equipped with a Diesel engine is considered. This choice is not restrictive, as the methodology presented here could be easily transposed to other cases of interest. The objective is to calculate, within a reasonable time, an eco-driving cycle for a HEV under final time, distance and SOC constraints while fulfilling the speed limits. We wish to find a trade-off between the accuracy of the DP solution and the complexity of the algorithms used to obtain this solution (an accuracy/complexity balance). For this purpose, four methods to calculate eco-driving cycles are considered:

- The first method is based on solving directly the optimal control problem associated to eco-driving for HEVs.

- The second method is based on reducing the number of state variables by introducing a tuning parameter to satisfy the SOC final constraint.

- The third method is based on decoupling the optimization of the control variables into two steps. In a first step, an eco-driving cycle is calculated assuming that the vehicle is propelled only by the engine. In the second step, to follow the calculated eco-driving cycle, an off-line energy management strategy is designed to optimize the torque split and the gear-box ratios.

- The last method is similar to the previous one where only the torque split is optimized in the second step.

These methods are compared in terms of fuel consumption, state trajectories, computation time of the DP and memory (RAM) use. Based on the numerical results, a conclusion about the chosen trade-off between accuracy/complexity is drawn.

The paper is organized as follows. In Section II, the vehicle model is described. The calculation of eco-driving cycles is detailed in Section III. Section IV details the proposed numerical methods to calculate eco-driving cycles for an HEV. Numerical and simulation results are discussed in Section V. In light of the results, some conclusions on the most convenient method to be used are drawn based on a trade-off between optimality/complexity.

2. Vehicle Modeling

The system considered here is a dual shaft parallel mild hybrid with an electric machine (*EM*) connected to the engine by a belt (Figure 1). The gearbox is between the power-train and the wheel. This architecture allows regenerative braking (the electric machine works as a generator during braking phases), hybrid and zero-emission vehicle (ZEV) modes. Due to the architecture choice, during the ZEV mode, the engine injection is cut off and the electric machine produces power, keeping the engine rotating. This system was used in (Michel et al., 2015; Simon et al., 2015).
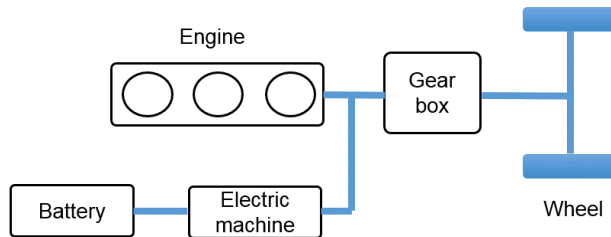

Figure 1: Parallel mild-hybrid architecture

2.1. Motion equations

The vehicle is modeled in a vertical plane. According to Newton's law of motion, the vehicle speed v satisfies the following differential equation

$$m \cdot \frac{dv(t)}{dt} = F_t(t) - F_r(t), \tag{1}$$

where F_t is the traction force to be provided by the engine, F_r is the sum of resistance forces and m is the total vehicle mass including the rotating parts. The force F_r comprises the rolling resistance force, the aerodynamic

drag force. Its expression is given by

$$F_r(t) = c_0 + c_1 \cdot v(t) + c_2 \cdot v(t)^2, \tag{2}$$

where c_i, $i = \{0, 1, 2\}$ are the constant coefficients of the road load equation. To take the road grade α into account, the coefficient c_0 will be not constant and its expression will be

$$c_0 = c_0^a + m \cdot g \cdot sin(\alpha), \tag{3}$$

where g is the acceleration of gravity, c_0^a is the road load coefficient. This model considers only the forces in the longitudinal direction. In this study, the road grade is null.

2.2. Internal Combustion Engine (ICE)

The ICE under consideration is a Diesel engine. The fuel consumption $\dot{m}_f$ (g/s) is computed through a look-up table as a function of the engine rotational speed (ω_{eng}) and the effective engine torque (T_{eng}) (see Figure 2)

$$\dot{m}_f = \dot{m}_f(\omega_{eng}, T_{eng}). \tag{4}$$

2.3. Electric machine model

The electric machine is modeled by a quasi-static map describing its electric power. The electric power P_m consumed (in traction mode) or supplied to the battery (in recuperation mode) is of the form

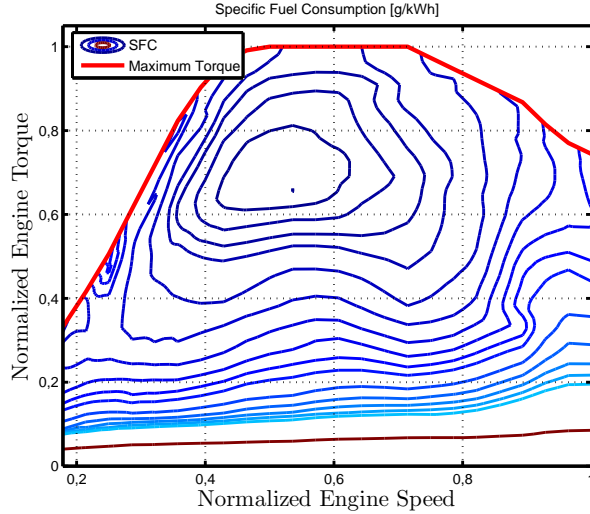$$P_m = P_m(\omega_{el}, T_{el}), \tag{5}$$

7

Figure 2: Specific fuel consumption SFC (g/kWh) of the ICE as a function of engine rotational speed and engine torque. For confidentiality reasons, the data are normalized.

where T_{el} is the electric machine torque and w_{el} is the electric machine rotational speed. This map includes the losses in the electric machine and the power electronic devices. The electric machine torque is limited by speed-dependent upper and lower bounds of the form (bold blue and black lines in Figure 3)

$$T_{elmin}(\omega_{el}) \leq T_{el} \leq T_{elmax}(\omega_{el}). \tag{6}$$

2.4. Battery model

The battery of Li-ion type is represented by an equivalent circuit model comprising a voltage source U_{ocv} in series with an electric resistance R_{bat}, both of which vary with ξ, the battery state of charge (SOC) (Guzzella and
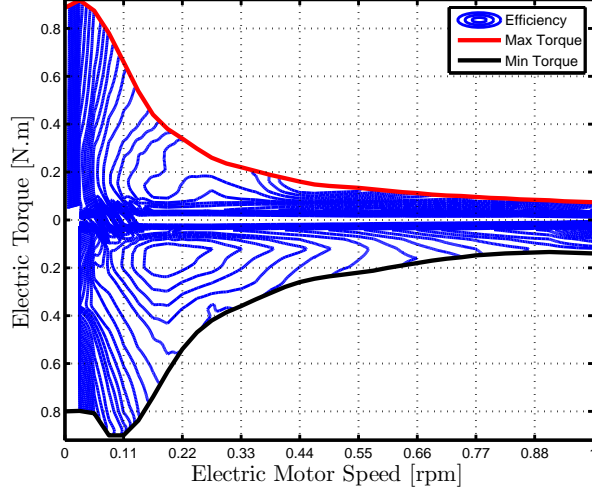
Figure 3: Electric Machine Efficiency as a function of the electric machine rotational speed and torque. For confidentiality reasons, the data are normalized.

Sciarretta, 2013; Badin, 2013). The expression of the battery current I_b is

$$I_b = \frac{1}{2R_{bat}(\xi)} \left(U_{ocv}(\xi) - \sqrt{U_{ocv}^2(\xi) - 4R_{bat}(\xi) \cdot P_b} \right), \tag{7}$$

where U_{ocv} and R_{bat} are given by look-up tables as functions of ξ (see Figures 4 and 5) and P_b is the power requested from the battery given by

$$P_b = P_m. \tag{8}$$

In reality, U_{ocv} and R_{bat} depend also on the battery mode (discharging or charging). These dependencies are neglected in this study as they will not impact the conclusion of the conducted analysis. The same battery model is used for what follows. The battery current I_b is also limited by its minimum value in the case of charging operation and its maximum value in the case of discharging phases. The dynamics of ξ is given by
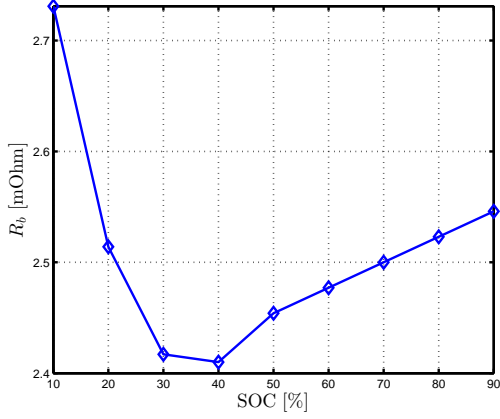
9

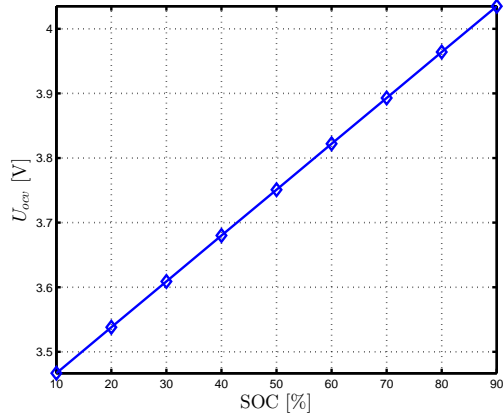Figure 4: Internal resistance R_{bat} [mΩ]   Figure 5: U_{ocv} [V]

$$\frac{d\xi(t)}{dt} = -\frac{I_b(t)}{Q_0}, \tag{9}$$

where Q_0 is the nominal battery capacity. In order to simplify the notation, the dynamics of ξ considering a given initial condition ξ_0 is written as

$$\frac{d\xi(t)}{dt} = g(v(t), \xi(t), T_{el}(t)), \ \xi(0) = \xi_0. \tag{10}$$

The inner (electrochemical) battery power is defined by

$$P_{ech}(v, \xi, T_e) = I_b(v, \xi, T_{el}) \cdot U_{ocv}(\xi). \tag{11}$$

2.5. Transmission

The engine torque T_{eng} and the electric machine torque T_{el} are related to the torque required at the wheel T_{wh} by

$$T_{wh}(t) = \eta_{gb} \cdot R_{gb}(t) \cdot R_t \cdot \left[T_{eng}(t) + R_{el} \cdot T_{el}(t)\right], \tag{12}$$

where R_{gb} is the gear-box ratio, r_{tire} is the wheel radius, η_{gb} is the gear-box efficiency (assumed to be constant), R_{el} is the constant motor-to-wheel transmission ratio and R_t is the differential ratio.

10

In the case of a conventional vehicle (with only an ICE), T_{wh} can be calculated using the formula

$$T_{wh}(t) = \eta_{gb} \cdot R_{gb}(t) \cdot R_t \cdot T_{eng}(t). \tag{13}$$

During braking phases, the maximum energy allowed by the electric machine is recovered and is used to recharge the battery. The remaining part is dissipated by the braking system.

Similarly, the rotational speed ω_{eng} of the ICE and ω_{el} of the electric machine are related to the vehicle speed v by

$$\omega_{el}(t) = R_{el} \cdot \omega_{eng}(t) = R_{gb}(t) \cdot R_t \cdot R_{el} \cdot \frac{v(t)}{r_{tire}}. \tag{14}$$

The model parameters are summarized in Table 1. The coefficients of the road load equations are omitted for confidentiality reasons.

3. Problem formulation

For a fixed road, the eco-driving methodology consists of finding the best speed profile minimizing the vehicle power consumption knowing that the vehicle starts from a point A at a given speed v_0 (≥ 0) and must reach a destination point B at time t_f, with a velocity v_1 (≥ 0). For an HEV, an additional constraint on the final SOC value is introduced. This constraint allows the comparison of many solutions by guaranteeing that they reach the same level of battery energy at the end of the driving cycle (Guzzella and Sciarretta, 2013; Sciarretta et al., 2004). This problem can be solved using optimal control tools (Mensing et al., 2014; Petit and Sciarretta, 2011).

11

Table 1: Vehicle model parameters

	Description	Value	Unit
m	Vehicle mass	1930	kg
r_{tire}	Wheel radius	0.34	m
η_{gb}	Gear-box efficiency	0.87	$-$
R_{gb}	Gearbox ratios	6	$-$
R_t	Differential ratio	3.53	$-$
R_{el}	Motor-to-wheel ratio	2.5	$-$
ω_{idle}	Engine idle speed	750	rpm
ω_{min}	min engine speed	750	rpm
ω_{max}	max engine speed	4000	rpm
ω_{elmax}	max electric machine speed	10000	rpm
ξ_{min}	SOC min value	20	%
ξ_{max}	SOC max value	90	%
a_{min}	Acceleration min value	-2	m/s^2
a_{max}	Acceleration max value	1.5	m/s^2

3.1. Optimal Control Problem (OCP) formulation

The cost function to be minimized is the fuel consumption over a fixed time window of duration t_f

$$J = \int_0^{t_f} \dot{m}_f(\omega_{eng}(t), T_{eng}(t))dt. \tag{15}$$

The control variable u is composed of three components: the engine torque T_{eng}, the electric machine torque T_{el} and the gear-box ratio R_{gb}

$$u(t) = [T_{eng}(t),\ T_{el}(t),\ R_{gb}(t)]. \qquad (16)$$

This optimization is carried out under the following dynamical constraints

$$\frac{dx(t)}{dt} = v(t), \qquad\qquad x(0) = 0, \qquad (17)$$

$$\frac{dv(t)}{dt} = f(v(t), u(t)), \qquad v(0) = v_0, \qquad (18)$$

$$\frac{d\xi(t)}{dt} = g(v(t), \xi(t), u(t)), \ \xi(0) = \xi_0, \qquad (19)$$

where x is the vehicle position and f is calculated by combining (1, 2, 12)

$$f = \frac{1}{m}[-c_0 - c_1 \cdot v - c_2 \cdot v^2 + \frac{\eta_{gb}}{r_{tire}} \cdot R_{gb} \cdot R_t \cdot (T_{eng} + R_{el} \cdot T_{el})]. \qquad (20)$$

Since the vehicle speed, the battery state of charge, the engine torque and speed, the electric machine torque and speed and the gear-box ratio are limited, and the final position, final speed and the final value of ξ are fixed,

the optimization must be performed under the following constraints

$$v(t) \in [0, \ v_{max}(x)], \tag{21}$$

$$f(v, u) \in [a_{min}, \ a_{max}], \tag{22}$$

$$\xi(t) \in [\xi_{min}, \ \xi_{max}], \tag{23}$$

$$T_{eng}(t) \in [T_{min}(\omega_{eng}(t)), \ T_{max}(\omega_{eng}(t))], \tag{24}$$

$$\omega_{eng}(t) \in [\omega_{min}, \ \omega_{max}], \tag{25}$$

$$T_{el}(t) \in [T_{elmin}(\omega_{el}(t)), \ T_{elmax}(\omega_{el}(t))], \tag{26}$$

$$\omega_{el}(t) \in [\omega_{elmin}, \ \omega_{elmax}], \tag{27}$$

$$x(t_f) = D, \tag{28}$$

$$v(t_f) = v_1, \tag{29}$$

$$\xi(t_f) = \xi_t, \tag{30}$$

where D is the total traveled distance, ξ_t is the desired final SOC, ξ_{min} and ξ_{max} are fixed values. The limitations T_{min}, T_{max}, T_{elmin} and T_{elmax} are given by look-up tables as a function of the engine speed ω_{eng} and the electric machine speed ω_{el}.

The speed limitations v_{max} in (21) are given as a function of the vehicle position and not of time (Mensing et al., 2011; Dib et al., 2014). In this study, the considered initial and final values of the vehicle speed are zero

$$v_0 = v_1 = 0. \tag{31}$$

Equation (22) limits the vehicle acceleration between its maximum and minimum values. The acceleration is an algebraic function of the vehicle speed and the control variables. This function can be evaluated for all the

14

possible choices of the vehicle speed and the control variables. The values not satisfying the constraint on the acceleration are excluded.

The constraints on the engine torque in (24) and the electric machine torque in (26) are mixed input-state constraints, they depend on the vehicle speed v and the gear-box ratio. The constraints on the rotational speeds in (25) and (27) are mixed input-state constraints, they depend on the vehicle speed and the gear-box ratio.

For the battery, the current I_b is limited between its maximum and minimum values in the case of battery charging and discharging. This constraint is not considered in the problem formulation. It will be checked a posteriori.

To summarize, the OCP considered in this paper is

$$(OCP): \quad \min_{u} \int_0^{t_f} \dot{m}_f(v, u) dt \tag{32}$$

under the dynamics (17, 18, 19), the state and input constraints (21, 22, 23, 24, 25, 26, 27), and the final constraints (28, 29, 30).

3.2. Speed limitations

To compute an eco-driving cycle from a given driving cycle, the following constraints (Mensing et al., 2014) have to be included:

- the same final distance $x(t_f)$, the same number of stops and the same duration t_f as the initial driving cycle,

- the vehicle speed limitations depending on the vehicle position x.

In this study, to specify the speed limits, a certain (fixed) margin e_l on the initial driving cycle speed is considered

$$v_{max}(x) = \begin{cases} v(x) + e_l, & v(x) > 0, \\ 0, & v(x) = 0, \end{cases} \qquad (33)$$

where $v(x)$ is the speed value of the initial cycle at the position x. Other types of limits can be considered as in (F. Mensing, 2013; Bouvier et al., 2015), where a set of legal speed limits v_{lim} were used. The process of identifying the speed limit for a given position x can be described in two steps:

1. find index j for which $v_{lim}(j-1) + e_l < v(x)$ and $v_{lim}(j) + e_l \geq v(x)$.
2. $v_{max}(x) = v_{lim}(j)$.

The choice of speed limits does not impact the solving method. Then, the objective is to find a new speed trajectory that takes these constraints into account and leads to a lower fuel consumption.

4. Solving Methods

The solution considered here is based on Dynamic Programming (DP) (Bertsekas, 2012). It is well-known that the number of the state and the control variables greatly impacts the numerical methods. Considering additional state and control variables increases the level of complexity and the computational burden. It may also jeopardize the robustness of numerical methods employed to compute the optimal trajectories.

In order to reduce the computation time, the method suggested in (F. Mensing, 2013; Bouvier et al., 2015; Monastyrsky and Golownykh, 1993) is

16

used, where the time-based OCP (with a fixed time step Δt) is transformed into a space-based OCP (with a fixed distance step Δx) using

$$\frac{d}{dt} = v \cdot \frac{d}{dx}.$$ (34)

In the space-based OCP, the stop phases are removed from the driving cycle. A comparison between the time-based and the space-based OCP solutions for a conventional vehicle is given in (Maamria et al., 2016b). If the position space is discretized in N points with a fixed step Δx, the time step $\Delta t(k)$, $k = 1 : N$ is variable and is *implicitly* calculated from the vehicle speed $v(k)$ and the vehicle acceleration $a(k)$ by solving the second order equation

$$\Delta x = \frac{1}{2} a(k) \cdot \Delta t(k)^2 + v(k) \cdot \Delta t(k).$$ (35)

The acceleration $a(k)$ is calculated from the vehicle speed $v(k)$ and the control variables $u(k)$. The final constraint on the vehicle position (28) is fulfilled by construction ($D = N \cdot \Delta x$). An additional tunable term $\beta \cdot \Delta t(k)$ is added to the cost function as a terminal cost: β penalizes the final time to obtain almost the same time duration as the initial driving cycle. The state variable x is omitted from the OCP (32). To calculate the right value of β, a root-finding method can be used to drive the final time error to zero as done in (Mensing et al., 2011; Sciarretta et al., 2015).

Based on this simplification, four methods to calculate eco-driving cycles for HEVs are defined in a *decreasing complexity order* as follows:

4.1. Method 1

In this method, the optimal control problem to be solved is the OCP described in (32) with the introduction of the tunable term $\beta \cdot \Delta t(k)$ in the

17

cost function as a terminal cost. The OCP has two state variables (v, ξ) and three control variables $(T_{eng}, T_{el}, R_{gb})$. The cost function to be minimized is

$$\sum_{k=1}^{k=N} [\dot{m}_f(v(k), u(k)) + \beta] \cdot \Delta t(k) \qquad (36)$$

under the dynamics (18, 19), the state and input constraints (21, 22, 23, 24, 25, 26, 27), and the final constraints (29, 30). The parameter β controls the duration of the trip t_f: it has been shown that the relations between β and t_f is monotonic. This method is denoted by (M_1) and it is considered as a reference of comparison in this study.

4.2. Method 2

The dynamic of ξ has been considered in the OCP (32) because of the final constraint (30). Moreover, it has been shown, by using the Pontryagin Minimum Principle (PMP) (Pontryagin et al., 1962), in the energy management system design for HEVs that neglecting the dependance of U_{ocv} and R_{bat} in ξ leads to a quasi-optimal fuel consumption (Serrao et al., 2011; Sciarretta et al., 2004; Kim et al., 2011). Thus, to reduce the number of state variables from 2 (v, ξ) to 1 (v), a new tunable quantity is added to the cost function (36) as follows

$$\sum_{k=1}^{k=N} \left[\dot{m}_f(v(k), u(k)) + \beta + \frac{\mu}{H_{lhv}} P_{ech}(v(k), \bar{\xi}, u(k)) \right] \cdot \Delta t(k), \qquad (37)$$

where H_{lhv} is the lower heating value of the fuel and $\bar{\xi}$ is a fixed value of ξ used to calculate mean (constant) values of R_b and U_{ocv} in the expression of the electrochemical power P_{ech} defined in equation (11). The parameter μ is used to bring the final SOC to its target value ξ_t: *for a fixed value of β, the*

18

relation between the final SOC and μ is monotone. Because of the absence of information about ξ in the backward loop, the instantaneous constraint (23) cannot be handled. This method was suggested in (F. Mensing, 2013; Bouvier et al., 2015) and it is denoted, in what follows, by (M_2).

4.3. Method 3

The third method (M_3) is based on decoupling the optimization of the control variables. The method involves two steps:

1. *Step1*: An eco-driving cycle is calculated assuming that the vehicle is propelled only by the ICE (vehicle parameters such as the weight and the road load coefficients do not change). The cost function to be minimized is the fuel consumption. The state variable is the vehicle speed v and the control variables are the engine torque T_{eng} and the gear-box ratio R_{gb}. The torque required at the wheel T_{wh} is related to T_{eng} and R_{gb} by the relation (13). The associated OCP is

$$\min_{(T_{eng},R_{gb})} \sum_{k=1}^{k=N} [\dot{m}_f(\omega_{eng}(k), T_{eng}(k)) + \beta] \cdot \Delta t(k) \qquad (38)$$

under the dynamics (18), the state and input constraints (21, 22, 24, 25, 26, 27), and the final constraints (29). The tunable parameter β penalizes t_f to obtain almost the same duration as the initial driving cycle. The expression of f in the dynamics of v, for this case, is

$$f = \frac{1}{m}[-c_0 - c_1 \cdot v - c_2 \cdot v^2 + \frac{\eta_{gb}}{r_{tire}} \cdot R_{gb} \cdot R_t \cdot T_{eng}]. \qquad (39)$$

This problem was studied in (F. Mensing, 2013; Sciarretta et al., 2015; Maamria et al., 2016b; Hooker, 1988; Ozatay et al., 2014; Kamal et al., 2010).

19

2. *Step2*: Using the DP, an energy management strategy is calculated for the eco-driving cycle obtained in *Step1*. For this purpose, the vehicle is assumed to follow the eco-driving cycle (the torque at the wheel T_{wh} is imposed). The objective is to determine the torque split between the electric machine and the ICE and the gear-box ratio in order to minimize the fuel consumption. The state variable is ξ with its final constraint (30). The control variables are the engine torque T_{eng} and the gear-box ratio R_{gb}. As the torque T_{wh} is imposed, the electric machine torque T_{el} is calculated from the torque balance in (12). On the other hand, the engine and the electric machine speeds are free as the gear-box ratio is considered as a control variable. They are calculated using formula (14) where only the vehicle speed v is known. The associated OCP can be written

$$\min_{(T_{eng}, R_{gb})} \sum_{k=1}^{k=N} \dot{m}_f(w_{eng}(k), T_{eng}(k)) \cdot \Delta t(k) \tag{40}$$

under the dynamics (19), state and input constraints (23, 24, 25, 26, 27), and the final constraints (30). The final time t_f is fixed (the duration of the eco-driving cycle in Step1). The PMP can not be used to solve the OCP (40) because the cost function is not convex with respect to the discrete control variable R_{gb} (Nesch et al., 2014).

4.4. Method 4

This last method (M_4) is also based on decoupling the optimization of the control variables into two steps:

1. *Step1*: This step is the same as *Step1* in Section 4.3.

20

2. *Step2*: Using the DP, an energy management strategy is calculated for the eco-driving cycle obtained in *Step1*. This step is similar to Step 2 in Section 4.3 where the gear-box ratio is fixed (Guzzella and Sciarretta, 2013; Serrao et al., 2011; Sciarretta et al., 2004; Kim et al., 2011). The control variable is the engine torque T_{eng}. As the torque T_{wh} is imposed, the electric machine torque T_{el} is calculated from the torque balance in (12). On the other hand, the engine and the electric machine speeds are imposed as the gear-box ratio is *fixed*. They are calculated using formula (14) where the vehicle speed v and the gear-box ratio R_{gb} are known. The associated OCP can be written

$$\min_{T_{eng}} \sum_{k=1}^{k=N} \dot{m}_f(\omega_{eng}(k), T_{eng}(k)) \cdot \Delta t(k) \tag{41}$$

under the dynamics (19), the state and input constraints (23, 24, 26), and the final constraints (30).

A similar approach was suggested in (Sciarretta et al., 2015; Ngo et al., 2010) where the second step was performed using the PMP (Pontryagin et al., 1962). Convex optimization can also be used for the second step (Nesch et al., 2014).

The number of state and control variables and the parameters to be tuned for each method are summarized in Table 2. The objective of this study is to find a trade-off between the optimality of the solution (fuel consumption), the number of parameters to be tuned and the computation time of the DP(s).

Table 2: Difference between tested methods: state, control variables and tuning parameters.

	States variables	Control variables	Tuning parameters
M_1	$2(v, \xi)$	$3(T_{eng}, T_{el}, R_{gb})$	$1\ (\beta)$
M_2	$1(v)$	$3(T_{eng}, T_{el}, R_{gb})$	$2\ (\beta, \mu)$
M_3	$1(v) + 1(\xi)$	$2(T_{eng}, R_{gb}) + 2(T_{eng}, R_{gb})$	$1\ (\beta)$
M_4	$1(v) + 1(\xi)$	$2(T_{eng}, R_{gb}) + 1(T_{eng})$	$1\ (\beta)$

5. Numerical Results

Six normalized driving cycles are considered: ECE-15 (the urban driving cycle), EUDC (the Extra-urban driving cycle), NEDC (the New European driving cycle), WLTC (the Worldwide harmonized Light vehicles Test Cycle), the low (LWLTC) and medium (MWLTC) phases of the WLTC. The *duration without stop phases*, the total traveled distance, mean speed value $\bar{v}$ and e$_l$ for each cycle are given in Table 3. *The stop phases are removed from the driving cycles. The optimization is performed only when the vehicle moves.*

The impact of the discretization step size on the optimality is not investigated. The study (Maamria et al., 2016b) addressed this question for conventional vehicles. Based on the results obtained, the step sizes for the vehicle speed, position and engine torque are chosen as follows: $\Delta v = 0.1$m/s for the vehicle speed, $\Delta x = 10$m for the distance in the case of ECE and LWLTC and $\Delta x = 20$m for the other driving cycles. For the control inputs u, steps of 2N.m for the engine and the electric machine torques are used. For the SOC, a step of $\Delta \xi = 0.25\%$ is used in the method (M_1) and of

Table 3: Driving cycle parameters

Cycle Name	Time [s]	Distance [km]	e_l [km/h]	$\bar{v}$ [km/h]
ECE-15	135	1.01	2	26.6
EUDC	360	6.9	4	69
MWLTC	386	5	3	46
LWLTC	445	2.98	1	24.1
NEDC	900	10.95	3	43.8
WLTC	1574	22.72	3	52

$\Delta\xi = 0.02\%$ in the second step of the methods (M_3) and (M_4). The initial value of the SOC is $\xi(0) = 60\%$. The gear-box considered has 6 ratios. The constraints on the battery current I_b are not considered in the problem formulation but checked in the forward computation (a posteriori).

For this study, a computer equipped with an Intel Core i7 2.30 GHz with 128 GB of RAM was used. The solution given by the method (M_1) is considered as a *reference of comparison*. However, this method is the most expensive in terms of Random-Access Memory (RAM) use and it is limited to three driving cycles: ECE, LWLTC and MWLTC (RAM saturation).

5.1. Optimality and computation time

The four methods are compared in terms of fuel consumption (Table 4), state trajectories, final time t_f and the desired final SOC for all the methods (Table 5), computation time for each iteration (Table 6) and the RAM use during the backward loop (Table 7).

In Table 4, the second and the third row (Init-conv and Init-HEV) give the

Table 4: Fuel consumption [g]

	ECE	EUDC	NEDC	LWLTC	MWLTC	WLTC
Init-conv	50.6	299.5	501.7	123.2	206.7	973.3
Init-HEV	33.2	283.8	414.8	91.1	178.4	829.3
(M$_4$)	21.6	229.3	317.3	69.1	122.5	665
(M$_3$)	20.7	227	310.9	67.4	120.8	655.9
(M$_2$)	20.5	226.6	310.3	66	118.3	649.1
(M$_1$)	20.3	—	—	65.9	118.2	—

fuel consumption for the initial driving cycles in the cases of a conventional and a hybrid vehicles (torque split only), respectively. They are used to assess the fuel saving of eco-driving for the considered methods.

Table 5: Final time [s] and the desired final SOC [%]

t_f	ECE	EUDC	NEDC	LWLTC	MWLTC	WLTC
M$_4$	134.9	360.8	900.3	434.4	385.1	1575.3
M$_3$	134.9	360.8	900.3	434.4	385.1	1575.3
M$_2$	134.3	360.2	900.3	434.4	385.8	1575.2
M$_1$	134.7	—	—	434.4	385.7	—
$\xi(t_f)$	60	60.21	60.39	60	59.97	60.21

From Table 5, the error on the final time for the tested methods is less than 0.7% with the same final SOC ($\xi(t_f)$). From Table 4 given the fuel consumption, it can be said that:

24

Table 6: Computation Time [s] for each iteration

	ECE	EUDC	NEDC	LWLTC	MWLTC	WLTC
M_4	6	29.7	47.8	17.3	17	104.6
M_3	63.6	228.1	415	171	159.1	707.5
M_2	50	368	596	144.5	171.4	1332
M_1	4300	–	–	11000	14600	–

- Methods (M_2) and (M_1) are close in terms of fuel consumption: sub-optimality less than 1% while computation time is divided by at least 85. This small difference is not surprising as the formulation of the method (M_2) is similar to a PMP transformation with a tunable parameter μ (for the EMS design using PMP, μ is the equivalence factor).

- The method (M_1) overloads the RAM, it uses at least 76GB.

Table 7: RAM use during backward loop [GB]

	ECE	EUDC	NEDC	LWLTC	MWLTC	WLTC
M_4	≤ 1	≤ 1	≤ 1	≤ 1	≤ 1	≤ 1
M_3	≤ 1	≤ 1	≤ 1	≤ 1	≤ 1	≤ 2
M_2	≤ 2	≤ 2	≤ 3	≤ 2	≤ 2	≤ 3
M_1	76	–	–	85	95	–

- The sub-optimality induced by using (M_3) compared to (M_2) is less than 2% while the computation times are close for short-driving cycles (ECE, LWLTC, MWLTC) and (M_3) is faster otherwise.

25

- The induced sub-optimality by using (M_4) compared to (M_2) is less than 3.5% except for the ECE case (where the error is 5%) while the computation time is divided by at least 8. The advantage of methods (M_3) and (M_4) compared to (M_2) is that only one parameter (β) has to be tuned. In the studies (F. Mensing, 2013; Monastyrsky and Golownykh, 1993; Maamria et al., 2016a), it was shown that, for conventional and electric vehicles, the relation between the final time t_f and β is monotone: t_f decreases when β increases.

- Fuel consumption reduction depends on the nature of the driving cycle. The fuel saving can be partially correlated to the mean speed $\bar{v}$ of the initial driving cycle: it increases when $\bar{v}$ decreases. It is the lowest for the EUDC while it is the highest for the ECE and the LWLTC.

5.2. Tuning of μ and β for the method (M_2)

For the method (M_2), two parameters have to be tuned, and thus at least two iterations are needed. Figures 6 and 7 show the sensitivity of t_f and the final SOC to β and μ for the LWLTC:

1. For a fixed value of β, the variation of t_f is small while the relation between the final SOC and μ is monotone: increasing the value of μ increases the final value of the SOC.

2. For a fixed value of μ, the variation of final SOC is small while the relation between the final time and β is monotone: increasing the value of β decreases t_f.

A similar analysis was conducted for other fixed values of β and μ and for the other driving cycles. These relations make the search for the *good*
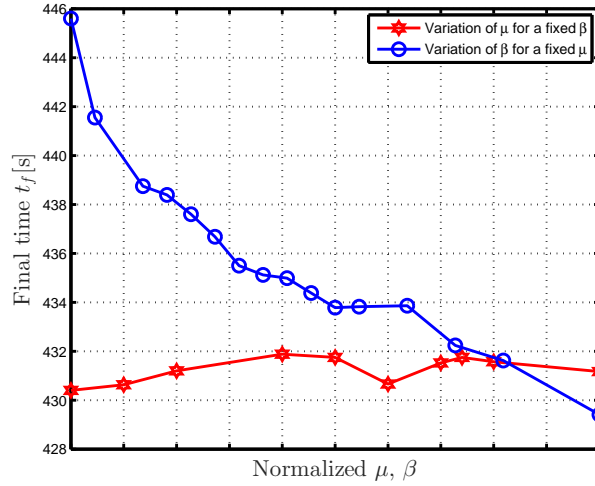
Figure 6: Sensitivity of the final time t_f: Method (M$_2$): real values are $\beta \in [0.45, \ 1]$ for fixed $\mu = 1.98$ and $\mu \in [1.8, \ 2.1]$ for fixed $\beta = 0.9$.
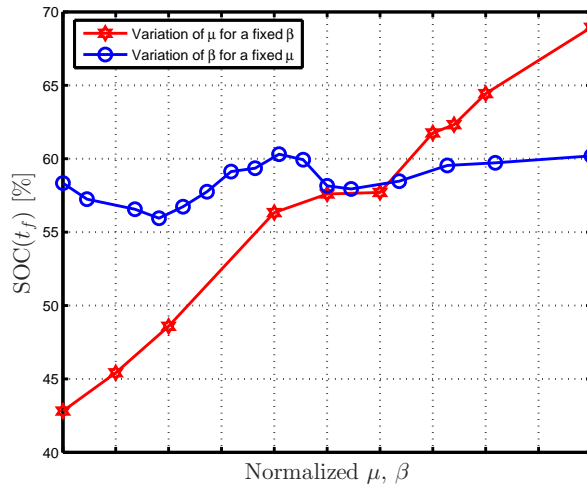

Figure 7: Sensitivity of SOC(t_f): Method (M$_2$): real values are $\beta \in [0.45, \ 1]$ for fixed $\mu = 1.98$ and $\mu \in [1.8, \ 2.1]$ for fixed $\beta = 0.9$.

values of β and μ easier. First, one can tune β to get a final time t_f near its target value. After, μ is tuned to bring the final SOC to its desired value.

The values of β and μ are adjusted iteratively.

5.3. State and control variables trajectories

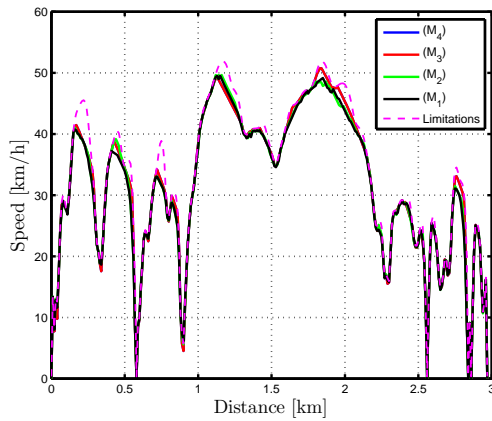The speed and SOC trajectories versus the distance for the LWLTC cycle are shown in Figures 8 and 9.
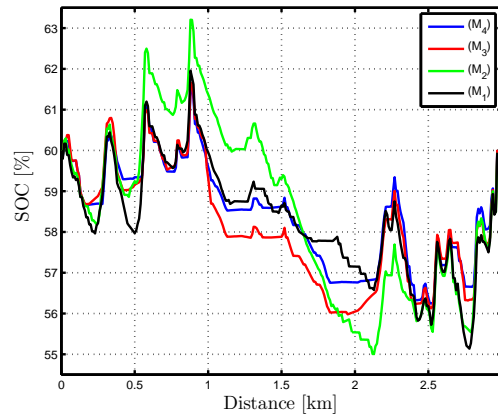

Figure 8: Vehicle speed [km/h] for LWLTC.   Figure 9: SOC [%] for LWLTC.

These figures show that the speed trajectories from methods (M_1) and (M_2) are very close. The main difference between (M_2) and $(M_{3,4})$ is in the deceleration phases. The same analysis is done for the other driving cycles: from the SOC trajectories in Figure 9, the different methods choose the same behavior: charging or discharging the battery. The methods (M_1) and (M_2) use the fact the vehicle is an HEV as this property is taken into account in the OCP formulation: Maximize the recharging phases. The methods (M_3) and (M_4) calculate, in a first step, an eco-driving cycle for a conventional vehicle, and thus, the braking system is hardly used as the deceleration and stop phases are anticipated.

To illustrate the difference between the tested methods, the operating points placement (rotating speed and torque) of the engine and the electric machine are given in Figures 10 and 11 for the driving cycle LWLTC. The axis labels are omitted for confidentiality reasons and a zoom is done. These two figures show that the operating points are very close.
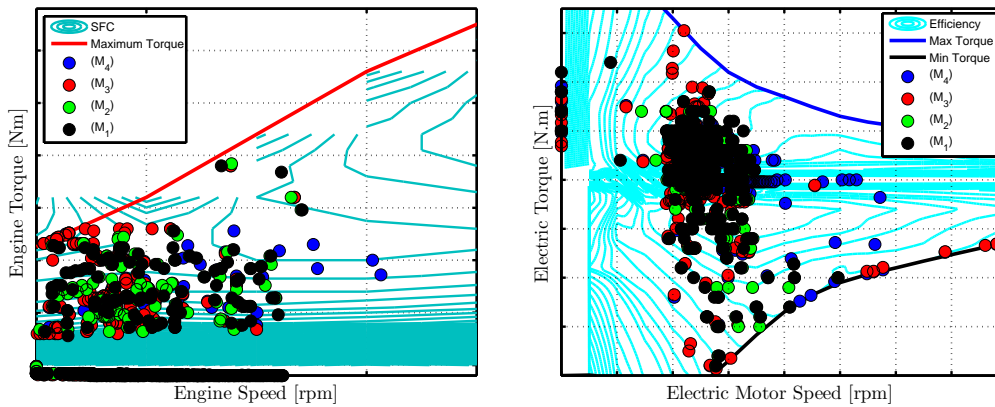

Figure 10: Engine operating points: LWLTC. Figure 11: (*EM*) operating points: LWLTC.

5.4. Summary of the study

The main objective of this study is to calculate, within a reasonable time, an eco-driving cycle for HEVs. The comparison of the tested methods in terms of fuel consumption reduction (with respect to fuel consumption of conventional vehicles), the normalized computation time (with respect to the computation time of the method (M_4)) and the RAM use is given in Figure 12. Based on these results, the methods (M_4) and (M_3) are the most suitable: the method (M_4) gives a *first good estimation* of the fuel saving with a *reasonable computation time*. By considering the gear-box optimization in
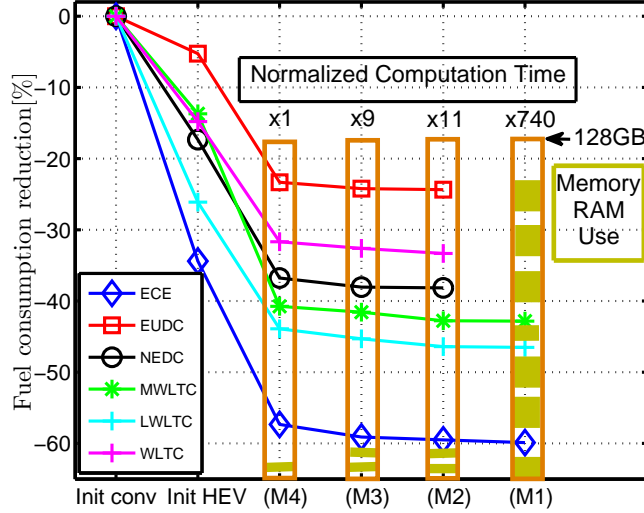
Figure 12: Summary: Methods comparison in terms of fuel consumption reduction [%], normalized computation time (with respect to (M_4)) and the RAM use.

(M_3), the induced sub-optimality is reduced to 2% while the computation time is still reasonable.

6. Conclusion

The calculation of eco-driving cycles for HEVs was studied. Four methods to solve the associated OCP were compared in terms of fuel consumption saving, state trajectories, computation time and memory (RAM) use with the objective of finding a trade-off between complexity and optimality. The result is that, for the parallel HEV under consideration, the simplest method, based on decoupling the optimization of the control variables into two steps, among all possible choices is accurate enough to guarantee a near optimal fuel saving (a sub-optimality of 3%) while ensuring a *reasonable* computa-

tion time. By considering the gear-box ratio as a degree of freedom in the energy management system optimization, the induced-sub-optimality is reduced to 1.5% while the computation time is multiplied by 10. The reference method (the most complicated) overloads the RAM (at least 70GB) and has an *inconvenient* computation time (compared to the simplest method). An intermediate method, based on reducing the number of state variable was also tested. Its drawback is the introduction of an additional tuning parameter.

References

Badin, F., 2013. Hybrid Vehicles. Editions TECHNIP.

Bertsekas, D., 2012. Dynamic programming and optimal control. Athena Scientific.

Bouvier, H., Colin, G., Chamaillard, Y., 2015. Determination and comparison of optimal eco-driving cycles for hybrid electric vehicles. European Control Conference, 142–147.

Dib, W., Chasse, A., Moulin, P., Sciarretta, A., Corde, G., 2014. Optimal energy management for an electric vehicle in eco-driving applications. Control Engineering Practice 29, 299–307.

F. Mensing, 2013. Optimal energy utilization in conventional, electric and hybrid vehicles and its application to eco-driving. Ph.D. thesis, INSA Lyon.

Guzzella, L., Sciarretta, A., 2013. Vehicle propulsion systems. Springer.

Heppeler, G., Sonntag, M., Sawodny, O., 2014. Fuel efficiency analysis for simultaneous optimization of the velocity trajectory and the energy manage-

ment in hybrid electric vehicles,. Proceedings of the 19th World Congress, 6612–6617.

Hooker, J., 1988. Optimal driving for single-vehicle fuel economy. Transportation Research-A, 183–201.

Kamal, M. A. S., Mukai, M., Murata, J., Kawabe, T., 2010. On board eco-driving system for varying road-traffic environments using model predictive control. IEEE International Conference on Control Applications, 1636–1641.

Kim, N., Cha, S., Peng, H., 2011. Optimal control of hybrid electric vehicles based on pontryagins minimum principle. IEEE Transactions on Control Systems Technology 19, 1279–1287.

Kim, T. S., Manzie, C., Sharma, R., 2009. Model predictive control of velocity and torque split in a parallel hybrid vehicle. IEEE International Conference on Systems, Man and Cybernetics, 2014–2019.

Maamria, D., Gillet, K., Colin, G., Chamaillard, Y., Nouillant, C., 2016a. On the use of dynamic programming in eco-driving cycle computation for electric vehicles. IEEE MSC.

Maamria, D., Gillet, K., Colin, G., Chamaillard, Y., Nouillant, C., 2016b. Which methodology is more appropriate to solve eco-driving optimal control problem for conventional vehicles? IEEE MSC.

Mensing, F., Bideaux, E., Trigui, R., Ribet, J., Jeanneret, B., 2014. Eco-driving: an economic or ecologic driving style? Transportation Research Part C: Emerging Technologies 38, 110–121.

Mensing, F., Trigui, R., Bideaux, E., 2011. Vehicle trajectory optimization for application in eco-driving. IEEE Vehicle Power and Propulsion Conference, 1–6.

Michel, P., Charlet, A., Colin, G., Chamaillard, Y., Bloch, G., Nouillant, C., 2015. Optimizing fuel consumption and pollutant emissions of gasoline-hev with catalytic converter. Control Engineering Practice.

Miyatake, M., Kuriyama, M., Takeda, Y., 2011. Theoretical study on eco-driving technique for an electric vehicle considering traffic signals. in Proc. 9th IEEE Int. Conf. Power Electronics Drive Systems, 733–738.

Monastyrsky, V., Golownykh, I., 1993. Rapid computation of optimal control for vehicles. Transportation Research Part B 27, 219–227.

Nesch, T., Elbert, P., Flankl, M., Onder, C., Guzzella, L., 2014. Convex optimization for the energy management of hybrid electric vehicles considering engine start and gearshift costs. ENERGIES 7, 834–856.

Ngo, D. V., Hofman, T., Steinbuch, M., Serrarens, A. F. A., 2010. An optimal control-based algorithm for hybrid electric vehicle using preview route information. Proceedings of the 2010 American Control Conference, 5818–5823.

Ozatay, E., Ozguner, U., Michelini, J., Filev, D., 2014. Analytical solution to the minimum energy consumption based velocity profile optimization problem with variable road grade. 19th World Congress, 7541–754.

Petit, N., Sciarretta, A., 2011. Optimal drive of electric vehicles using

an inversion-based trajectory generation approach. 18th IFAC World Congress 18, 14519–14526.

Pontryagin, L.-S., Boltyanskii, V.-G., Gamkrelidze, R.-V., Mishchenko, E.-F., 1962. The mathematical theory of optimal processes. Interscience Publishers John Wiley & Sons, Inc. New York, London.

Sciarretta, A., Back, M., Guzzella, L., 2004. Optimal control of parallel hybrid electric vehicles. IEEE Transactions on Control Systems Technology 12 (3), 352–363.

Sciarretta, A., Nunzio, G. D., Ojeda, L. L., 2015. Optimal ecodriving control: Energy-efficient driving of road vehicles as an optimal control problem. IEEE Control Systems Magazine 35.5, 71–90.

Serrao, L., Onori, S., Sciarretta, A., Guezennec, Y., Rizzoni, G., 2011. Optimal energy management of hybrid electric vehicles including battery aging. American Control Conference.

Simon, A., Michel, P., Nelson-Gruel, D., Chamaillard, Y., 2015. Gasoline-hev equivalent consumption and pollutant minimization strategy. IEEE Vehicle Power and Propulsion Conference.

van Keulen, T., de Jager, B., Foster, D., Steinbuch, M., 2010. Velocity trajectory optimization in hybrid electric trucks. in Proc. American Control Conference, 5074–5079.